Numerical simulation of the deformation of charged drops of electrolyte

M. R. Davidson[1], J. D. Berry[1,2] & D. J. E. Harvie[1]
[1]*Department of Chemical and Biomolecular Engineering, The University of Melbourne, Australia*
[2]*CSIRO Computational Informatics, Australia*

Abstract

The volume-of-fluid based numerical method of Berry *et al.* (*J. Computational Physics*, 251, pp. 209–222, 2013), for predicting electrokinetic flow of multiphase flow with deformable interfaces, is extended to account for the effect of interfacial charge. The numerical representation of interfacial charge is validated using two simple test cases. Finally, the use of the extended algorithm is demonstrated by simulating the breakup of an unstable charged water drop in air.
Keywords: two-fluid flow, Volume of Fluid, charged interface, electrokinetic.

1 Introduction

The deformation of a drop in an electric field is a classical problem of electrohydrodynamics, with most theoretical studies assuming variously either a perfect dielectric or perfectly conducting drop, or the leaky dielectric model [2]. Over the last 25 years, numerical methods have been used increasingly to analyse aspects of the problem based on such assumptions. Techniques have included the boundary integral [3], finite element [4], front tracking [5], level-set (LS) [6], and volume-of-fluid (VOF) [7] methods.

The above models assume uniform permittivity and conductance within each fluid phase (drop fluid and surrounding fluid) so that all electyrohydrodynamic coupling occurs at the interface. However, in electrolytes, the ions in solution redistribute under the action of an electric field, resulting in a non-uniform charge distribution (and hence non-uniform conductance) within the bulk of each fluid. This electrokinetic behaviour due to mobile charge carriers was studied analytically by Zholkovskij *et al.* [8] for small drop deformation. Numerical


WIT Transactions on Engineering Sciences, Vol 82, © 2014 WIT Press
www.witpress.com, ISSN 1743-3533 (on-line)
doi:10.2495/AFM140181

modelling was extended by López-Herrera *et al.* [9] using a VOF method to include spatially varying charge and conductivity; however, the conductivity distribution required specification because the transport of individual species of charge carriers was not accounted for.

Recently, the authors developed a new numerical algorithm for calculating electrokinetic flow with fluid/fluid interfaces (Berry *et al.* [1]) that allows for the coupled calculation of convective, conductive and diffusive ion transport, and electrical potential distribution. Because the transport of individual ion species (charge carriers) is accounted for, the conductivity distribution is determined as part of the calculation. The new algorithm is based on a combined level-set, volume-of-fluid method [10].

Although the authors' new method [1] extends the modelling of electrohydrodynamic flow to include electrokinetic flow, the new procedure does not explicitly address situations in which the fluid/fluid interface is charged. Accounting for interface charge presents numerical challenges because of the associated jump in the electric displacement at the deforming interface. The aim of this paper is to extend the authors' algorithm to allow for interfacial charge, and to verify the numerical accuracy of its representation for drops and planar interfaces using test problems.

2 Formulation

Consider two immiscible Newtonian fluids with interfacial tension γ, comprising an electrolyte solution in contact with a fluid that contains no ions, where the interface carries charge density q that is taken to be uniform. The two fluids are termed the discrete phase and the continuous phase (e.g. a drop of electrolyte immersed in oil or in air, or conversely). The discrete and continuous phases are denoted by subscripts d and c, respectively. We further assume that the electrolyte contains symmetric cations and anions, denoted by $+$ and $-$ respectively, with equal diffusivities $D_+ = D_- = D$ and valencies $z_+ = -z_- = z$. The phases are assumed to have uniform viscosities $\mu_{(d,c)}$, densities $\rho_{(d,c)}$ and relative permittivities $\epsilon_{(d,c)}$. A reference concentration (number density) of ions is denoted by n_0, and is taken equal to the geometric mean of the ion concentrations [11]. The effect of gravity is ignored as is appropriate when the densities of the two fluids are closely matched, or when the typical length scale is very small (e.g. order of micrometers).

In terms of dimensionless variables, the governing equations for flow in a VOF-based formulation are [1]

$$\frac{\partial \rho \mathbf{v}}{\partial t} + \nabla\cdot(\rho\mathbf{v}\mathbf{v}) = -\nabla P + \frac{1}{\mathrm{Re}}\nabla\cdot\boldsymbol{\tau} + \frac{1}{\mathrm{We}}\mathbf{F}_\mathrm{s} + \frac{\mathrm{Ca_E}}{\mathrm{We}}\nabla\cdot\boldsymbol{\tau}_\mathrm{m} \tag{1}$$

$$\nabla\cdot\mathbf{v} = 0 \tag{2}$$

$$\frac{\partial \phi}{\partial t} + \nabla\cdot(\mathbf{v}\phi) = 0 \tag{3}$$

where

$$\boldsymbol{\tau}_{\mathrm{m}} = \epsilon \mathbf{E}\mathbf{E} - \frac{1}{2}\epsilon(\mathbf{E}\cdot\mathbf{E})\mathbf{I} \tag{4}$$

$$\mathbf{E} = -\nabla U \tag{5}$$

The corresponding VOF-based equations for the electric field and ion transport are [1]

$$\nabla\cdot(\epsilon\mathbf{E}) = \frac{1}{2}K^2(n_+ - n_-) + S_q \tag{6}$$

$$\frac{\partial \phi n_\pm}{\partial t} + \nabla\cdot\left(\phi n_\pm\left(\mathbf{v} \pm \frac{1}{\mathrm{Pe}}\mathbf{E}\right)\right) = \frac{1}{\mathrm{Pe}}\nabla\cdot(\phi\nabla n_\pm) \tag{7}$$

Here $\mathbf{v}$ is the fluid velocity vector, P denotes pressure, $\boldsymbol{\tau}$ is the viscous stress tensor, $\mathbf{F}_{\mathrm{s}}$ is the surface force arising from interfacial tension, $\boldsymbol{\tau}_{\mathrm{m}}$ denotes the Maxwell stress tensor associated with electrical forces on the fluid, ϕ is the fractional volume function for the discrete phase, $\mathbf{E}$ is the electric field, U is the electrical potential, and $n_\pm$ denotes the number densities of cations and anions. The source term S_q in eqn. (6) for the electric field denotes the contribution to the total charge per unit volume that arises from the interfacial charge density q.

The velocity has been non-dimensionalised according to a characteristic velocity scale V that will depend on the physical system under consideration. Length, time, number density of cations and anions, and electric field, have been scaled according to drop radius R, R/V, n_0 and $E_{\mathrm{ref}} = kT/zeR$, respectively, where k is the Boltzmann constant, T is the absolute temperature and e denotes the elementary charge. In addition, the density, viscosity and permittivity are scaled using corresponding fluid properties of the electrolyte phase, so that scaled values are unity within the electrolyte phase and a ratio of values in the other phase.

The resulting dimensionless groups in the governing equations are

$$\mathrm{Re} = \frac{\rho_{\mathrm{ref}} V R}{\mu_{\mathrm{ref}}}, \quad \mathrm{We} = \frac{\rho_{\mathrm{ref}} V^2 R}{\gamma}, \quad \mathrm{Ca_E} = \frac{\epsilon_0\epsilon_{\mathrm{ref}} E_{\mathrm{ref}}^2 R}{\gamma} \tag{8}$$

$$\mathrm{Pe} = \frac{VR}{D_{\mathrm{ref}}}, \quad K^2 = \frac{2z^2e^2n_0R^2}{\epsilon_0\epsilon_{\mathrm{ref}}kT} \tag{9}$$

where subscript 'ref' denotes a reference value and ϵ_0 is the permittivity of free space. The groups Re, We, Pe, and $\mathrm{Ca_E}$ are the Reynolds, Weber, Peclet, and electric capillary numbers, respectively, while K is the dimensionless inverse Debye length.

The source term S_q representing interfacial charge in eqn. (6) is absent in the formulation of Berry *et al.* [1] since they implicitly assume that the interface itself carries no charge. In order to use the numerical algorithm of Berry *et al.* [1] to solve the governing equations (1)–(7), a suitable representation for S_q is required.

3 Approximating the electric field equation

The electric field is determined by solving eqn. (6) which, in terms of the electrical potential U, is the Poisson equation

$$\nabla\cdot(\epsilon\nabla U) = -\frac{1}{2}K^2(n_+ - n_-) - S_q \tag{10}$$

A simple representation of S_q is

$$S_q = S_I\delta_I \tag{11}$$

where $\delta_I = |\nabla\phi|$ is the Dirac delta function centred at the interface and

$$S_I = \frac{zeRq}{\epsilon_0\epsilon_{\mathrm{ref}}kT} \tag{12}$$

is the dimensionless interfacial charge density. Although the electrical potential (U) is continuous at the interface, the potential gradient (electric field) is discontinuous there in general. Experience shows that the delta function formulation of S_q predicts a non-physical step change in U at the interface in the presence of interfacial charge, except when the permittivities of the two phases are equal.

In VOF or LS methods the location of the interface is not known precisely. If the interface location was known then the exact equations for the electrical potential would consist of eqn. (10) with $S_q = 0$ in each phase separately, linked at the interface by the following condition on the electrical displacement:

$$\|-\epsilon\nabla U\|\cdot\hat{\mathbf{n}} = S_I \tag{13}$$

where $\|\cdot\|$ indicates a jump across the interface and $\hat{\mathbf{n}}$ denotes a unit normal to the interface pointing opposite to the direction of the jump. A numerical method that is designed to solve problems such as this, incorporating the jump condition (13) and a discontinuity in ϵ, has been developed by Liu *et al.* [12]. The technique involves approximating gradients at points that are adjacent to the interface, by smoothly extending the solution in one phase to fictitious values across the interface. Implementation of the method of Liu *et al.* [12] yields a representation of S_q that differs from the delta function formulation (11), and it will be shown that the corresponding solution does not suffer from a non-physical jump in U at the interface that characterises the use of eqn. (11).

Applying the method of Liu *et al.* [12] yields the following expression for S_q at cell-centred nodal points with coordinates (x_i, y_j) on a uniform rectangular computational grid with mesh spacing Δx and Δy in the x and y coordinates, respectively:

$$S_q = -(F^L + F^R + F^B + F^T) \tag{14}$$

where F^L is non-zero when the interface lies between x_{i-1} and x_i, and F_R is non-zero when the interface lies between x_i and x_{i+1}. Likewise, F^B and F^T are

non-zero when the interface is located between y_{j-1} and y_j, and between y_j and y_{j+1}, respectively. At all other locations, F^L, F^R, F^B, F^T are zero. The non-zero values of F^L and F^R are given by:

$$F^L = \frac{\epsilon_{i-\frac{1}{2},j} S_I \hat{n}^{(1)} \theta_{i-1,j}}{\epsilon_d \Delta x} \tag{15}$$

when (x_{i-1}, y_j) lies within the discrete phase (fig. 1(a));

$$F^L = -\frac{\epsilon_{i-\frac{1}{2},j} S_I \hat{n}^{(1)} \theta_{i-1,j}}{\epsilon_c \Delta x} \tag{16}$$

when (x_i, y_j) lies within the discrete phase (fig. 1(b));

$$F^R = \frac{\epsilon_{i+\frac{1}{2},j} S_I \hat{n}^{(1)} \theta_{i+1,j}}{\epsilon_c \Delta x} \tag{17}$$

when (x_i, y_j) lies within the discrete phase (fig. 1(c));

$$F^R = -\frac{\epsilon_{i+\frac{1}{2},j} S_I \hat{n}^{(1)} \theta_{i+1,j}}{\epsilon_d \Delta x} \tag{18}$$

when (x_{i+1}, y_j) lies within the discrete phase (fig. 1(d)).

Here $\theta_{i\pm1,j}\Delta x$ is the distance along the x-coordinate between $(x_{i\pm1}, y_j)$ and the interface, $\hat{n}^{(1)}$ is the x-component of the unit normal ($\hat{\mathbf{n}}$) to the interface directed into the discrete phase, and $\epsilon_{i\pm\frac{1}{2},j}$ is a θ-weighted harmonic average of ϵ evaluated at the mesh cell face between the nodes $(x_{i\pm1}, y_j)$ and (x_i, y_j) Analogous expressions apply for F^B and F^T.

Liu *et al.* [12] use a level-set function to represent $\theta_{i\pm1,j}$ and $\hat{\mathbf{n}}$, and to perform the averaging of ϵ to obtain $\epsilon_{i\pm\frac{1}{2},j}$. Here we approximate these instead using the VOF volume function ϕ. In that case

$$\hat{\mathbf{n}} = \frac{\nabla\phi}{|\nabla\phi|} \tag{19}$$

Furthermore, when discrete phase is to the left of the interface (figs. 1(a), 1(c)), we set

$$\theta_{i-1,j} = \phi_{i-\frac{1}{2},j} \tag{20}$$

$$\theta_{i+1,j} = 1 - \phi_{i+\frac{1}{2},j} \tag{21}$$

and when the discrete phase is on the right of the interface (figs. 1(b), 1(d)),

$$\theta_{i-1,j} = 1 - \phi_{i-\frac{1}{2},j} \tag{22}$$

$$\theta_{i+1,j} = \phi_{i+\frac{1}{2},j} \tag{23}$$

where $\phi_{i\pm\frac{1}{2},j}$ denotes the discrete phase volume fraction between nodes $(x_{i\pm1}, y_j)$ and (x_i, y_j). The component $\hat{n}^{(1)}$ of the unit normal to the interface is

approximated by a linearly interpolated value $\hat{n}^{(1)}_{i\pm\frac{1}{2},j}$ at the mesh cell face between the nodes $(x_{i\pm1}, y_j)$ and (x_i, y_j). The interpolation used here to obtain $\epsilon_{i\pm\frac{1}{2},j}$ using the VOF volume function, that corresponds to the treatment of Liu *et al.* [12], is the volume fraction weighted harmonic mean interpolation used by Berry *et al.* [1].

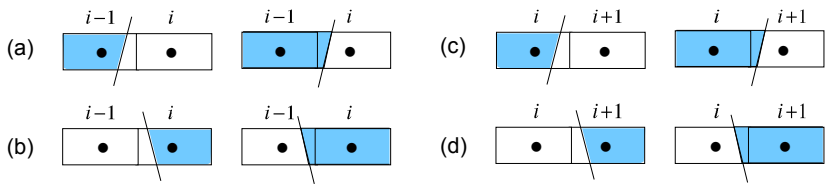

Figure 1: Schematics of an interface segment located (a, b) between nodal points x_{i-1} and x_i and (c,d) between nodal points x_i and x_{i+1}. The shaded region denotes drop fluid.

4 Results and discussion

We now consider two test cases chosen to test the extended algorithm when interfacial charge is represented by eqn. (11) (delta function method) or by eqn. (14) (method adapted from Liu *et al.* [12]). The complete set of governing equations (1)–(7) is solved numerically, even in cases where there should be no fluid motion. Calculations are performed on a two-dimensional uniform staggered grid. Further details of the numerical procedure are given in Berry *et al.* [1].

4.1 Test case: uniform layer of electrolyte

This case concerns a stationary uniform layer of electrolyte (taken to be the discrete phase) which is in contact with a solid wall on one side at $x = 0$, and a gas (e.g. air) on the other side at $x = 1$ (fig. 2). The wall is assumed to be charged with a dimensionless surface charge density $S_w = 4$, and the corresponding interface surface charge density is taken to be $S_I = -4$. The definition of S_w has the same form as for S_I (eqn. (12)), with the dimensional charge density on the wall replacing the interfacial quantity q. The permittivity ratio is specified to be $\epsilon_c/\epsilon_d = 0.0125$, and the dimensionless inverse Debye length is taken to be $K = 2$. Other parameters necessary to solve the complete set of governing equations (1 - 7) are specified as follows: density ratio $\rho_c/\rho_d = 0.001$, viscosity ratio $\mu_c/\mu_d = 0.003$, Re $= 1.0$, We $= 1.0$, Pe $= 1000$, $\mathrm{Ca_E} = 0.468 \times 10^{-3}$.

For a symmetric 1:1 electrolyte, the exact steady state governing equations for the electrical potential take the standard Poisson-Boltzmann form in one dimension:

$$\frac{d^2U_d}{dx^2} = K^2 \sinh U_d, \quad x \in (0,1) \tag{24}$$

$$\frac{d^2U_c}{dx^2} = 0, \quad x \in (1, \infty) \tag{25}$$

with boundary conditions

$$\left.\frac{dU_d}{dx}\right|_{x=0} = -S_w, \qquad \left.\frac{dU_c}{dx}\right|_{x\to\infty} = 0 \tag{26}$$

$$U_d|_{x=1} = U_c|_{x=1} \tag{27}$$

$$\varepsilon_d \left.\frac{dU_d}{dx}\right|_{x=1} - \varepsilon_c \left.\frac{dU_c}{dx}\right|_{x=1} = S_I \tag{28}$$

The ion concentrations are

$$n_\pm = \begin{cases} \exp(\mp U), & \text{if } x \le 1, \\ 0, & \text{if } x > 1 \end{cases} \tag{29}$$

High-resolution solutions (1000 points per unit length) to the one dimensional eqns. (24)–(29) are referred to as 'exact' solutions.

fig. 2 compares numerical solutions for this case, obtained using the method of Berry *et al.* [1], extended to include interface charge based on the delta function method (eqn. (11)) or the method adapted from Liu *et al.* [12] (eqn. 14)). Calculations are performed using 32 mesh cells per unit length with a computation domain extending to 2 dimensionless lengths transversely. The condition at infinity (zero potential gradient) is applied at $x = 2$, and the ion concentrations at $t = 0$ are set according to the exact solution. Numerical timestepping proceeds until steady state is achieved. The results are also compared with the exact solutions. fig. 2 shows that the method adapted from Liu *et al.* [12] accurately predicts the electrical potential variation. In contrast, the delta function method exhibits an unphysical step-change in the potential at the interface, although it correctly predicts the potential in the electrolyte ($x < 1$), and correctly predicts zero electrical field (potential gradient) in the gas away from the interface. Predictions of both methods and the exact solution for the positive and negative ion concentrations are effectively coincident (fig. 2b). No results for ion concentrations are shown for $x > 1$ because there are no ions in the gas phase. Both methods predict that the fluids remain stationary at all times, consistent with the exact solution.

4.2 Test case: two dimensional drop of electrolyte

In this case, we consider a stationary two dimensional drop of electrolyte (discrete phase) with radius $R = 1$, suspended in perfect dielectric liquid. The dimensionless surface charge density on the drop-liquid interface is taken to be $S_I = -4$, the permittivity ratio is specified to be $\epsilon_c/\epsilon_d = 0.025$, and the dimensionless inverse Debye length is taken to be $K = 5$. Other parameters necessary to solve the complete set of governing equations (1 - 7) are specified as follows: density ratio $\rho_c/\rho_d = 1.0$, viscosity ratio $\mu_c/\mu_d = 3$, Re $= 0.01$, We $= 2.0$, Pe $= 10$, $\mathrm{Ca_E} = 9.36$.

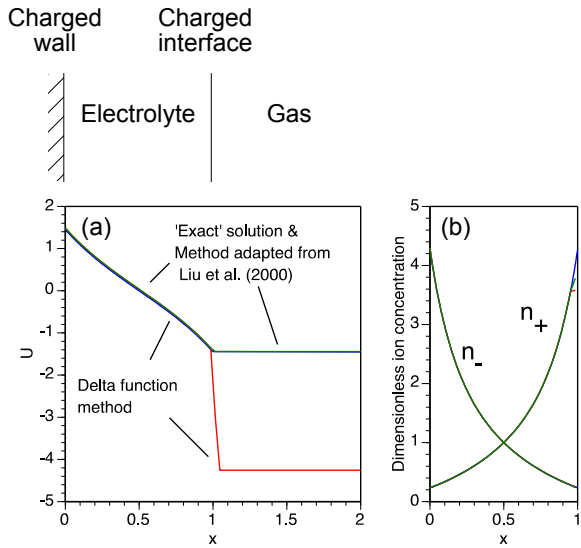

Figure 2: Test case: stationary uniform layer of electrolyte. Comparison of methods for representing interfacial charge (eqns. 11 and 14) when predicting (a) electrical potential and (b) ion concentrations at steady state. Here $S_w = 4$, $S_I = -4$, $\epsilon_c/\epsilon_d = 0.0125$, $K = 2$.

The exact steady state governing equations for the electrical potential and ion concentrations in terms of the planar polar radius r, when the drop consists of a 1:1 electrolyte, are similar to eqns. (24)–(29) but with r replacing x, S_w set to zero, and $\frac{1}{r}\frac{\partial}{\partial r}\left(r\frac{\partial U}{\partial r}\right)$ replacing $\frac{d^2U}{dx^2}$. We consider the circumstance in which the total charge due to ions inside the drop is equal and opposite to the total charge on the drop interface (i.e. overall electro-neutrality). A simple application of Gauss' law demonstrates that the potential must be constant outside the drop in this case.

For the numerical solution, we set the electro-neutrality by choosing the initial ion concentrations in the drop to be the average values in the drop evaluated from the exact solution (eqn. (29)). Since the drop is stationary and the interfacial area is not changing, this electro-neutrality condition should be satisfied at all later times for fixed interfacial charge density S_I.

The numerical solutions based on the two methods of representing surface charge are now compared in fig. 3 for this two dimensional drop case. Results are presented for electrical potential and ion concentration along the horizontal axis through the centre of the drop. The results are almost the same along the vertical axis, as is expected. The computation domain is a symmetric half-plane of width 4 and length 8 with the drop of radius equal to 1 located centrally (drop centre at $(0, 4)$). Again calculations are performed using 32 mesh cells per unit length. Zero potential gradient is specified at the boundaries of the computational domain.

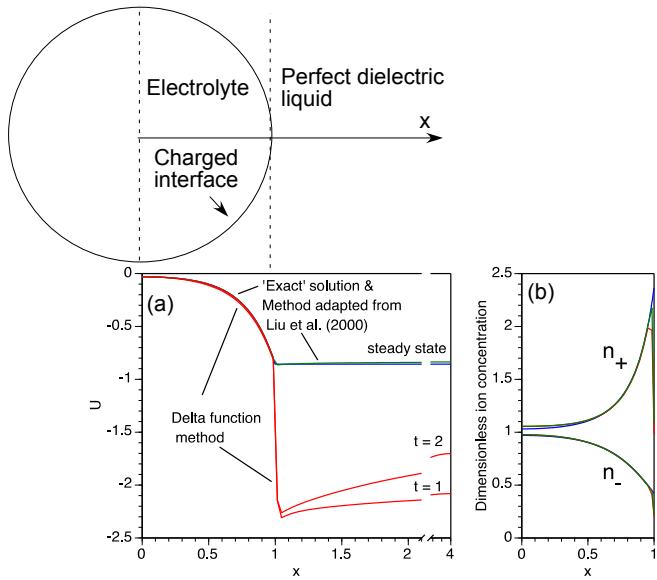

Figure 3: Test case: stationary planar drop of electrolyte. Comparison of methods for representing interfacial charge (eqns. 11 and 14) when predicting (a) electrical potential and (b) ion concentrations at $t = 1$ and $t = 2$ for the delta function method, and at steady state for the other method. Here $S_I = -4$, $\epsilon_c/\epsilon_d = 0.025$, $K = 5$.

As in the previous test case, the method adapted from Liu *et al.* [12] (eqn. (14)) for describing the interfacial charge, accurately predicts the electrical potential distribution, both inside and outside the drop, when compared with the exact solution. The delta function method is once more shown to exhibit an unphysical jump in the potential at the interface, while accurately predicting the potential variation inside the drop. However, in this case, the delta function method does not reproduce the correct (zero) potential gradient outside the drop. This deviation from the exact solution increases with time, as is shown by the results for $t = 1$ and $t = 2$, so that the delta function method never achieves a steady result throughout the domain. The reason for this error is explained below.

The unphysical step change in potential predicted at the interface by the delta function method results in a spike in the calculated electrical field there. This enhances the generation of unrealistic parasitic currents (not shown) that can occur near a curved interface when using LS and VOF methods. These exaggerated parasitic currents cause minute corrugations in the interface that grow with time, so that the calculated interfacial area grows with time. Consequently, the condition of overall electro-neutrality becomes increasingly in error as the calculation with the delta function method proceeds for fixed interfacial charge density S_I, resulting in

a non-uniform potential variation outside the drop that becomes more pronounced with time. This error does not occur with the method based on Liu *et al.* [12].

As for the previous test case, both methods accurately predict the ion concentrations when compared with the exact solution (fig. 3b). No ion concentrations are shown for $x > 1$ because there are no ions outside the drop.

4.3 Illustrative example

The above tests show that representing S_q using the procedure based on Liu *et al.* [12] can satisfactorily account for the effect of interfacial charge. We now illustrate the application of this method to the more physically interesting problem of breakup of a water drop in air when the charge Q on the drop surface exceeds the Rayleigh limiting value for stability, $Q_c = 8\pi\sqrt{\gamma\epsilon_0 R^3}$ [2]. Here we assume that the drop surface carries a fixed charge $Q = 1.05Q_c$, and that the drop contains no ions. As the unstable drop deforms, its area changes, thus changing the interfacial charge density. Charge migration on the drop surface is ignored, so that S_I remains uniform but changing with time. The physical parameters of the problem are $\rho_c/\rho_d = 0.001$, $\mu_c/\mu_d = 0.018$, $\epsilon_c/\epsilon_d = 0.0125$. The velocity scale is chosen so that We $= 1.0$ in which case Re $= 27.4$ and $\mathrm{Ca_E} = 0.62 \times 10^{-6}$, based on a spherical droplet of 10 micrometre radius.

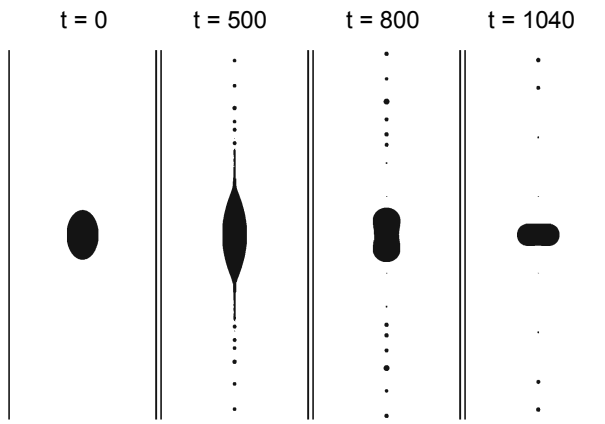

Figure 4: Time evolution of an initially deformed, charged unstable water drop in air. Interfacial charge is 1.05 times the critical Rayleigh value for instability. Here $\rho_c/\rho_d = 0.001$, $\mu_c/\mu_d = 0.018$, $\epsilon_c/\epsilon_d = 0.0125$, We $= 1.0$, Re $= 27.4$, $\mathrm{Ca_E} = 0.62 \times 10^{-6}$.

Calculation is performed for a drop that is initially deformed (fig. 4) on a grid having 32 mesh cells per unit length in a computation domain of radius equal to 4 drop radii and length of 16 drop radii. Refining the grid to 64 cells per unit length produced negligible change in the results. The electric field at points on the

domain external boundaries is chosen to be proportional to the inverse square of the spherical polar radius, consistent with the analytical solution outside a spherical drop having uniform potential. The constant of proportionality is chosen to satisfy Gauss' law throughout the domain. For this example only, the numerical solution of the momentum eqn. (1) is performed with a modified pressure that incorporates an additional term proportional to $\frac{1}{2}\epsilon\mathbf{E}^2$ deriving from the second term in eqn. (4). The drop evolution shown in fig. 4 is similar to that shown in experimental images of a related case [13]. Detailed investigation of this and similar problems using our numerical methods, including an exploration of the validity of the modified pressure treatment, will be the subject of future work.

5 Conclusion

The algorithm of Berry *et al.* [1] for calculating electrokinetic multiphase flow with interfaces is extended here to include the effect of interfacial charge. Two numerical representations of the interfacial charge are compared. One uses the Dirac delta function centred at the interface, and the other is based on a technique developed by Liu *et al.* [12] for solving Poisson's equation with jump conditions at an interface. Two test problems (a uniform electrolyte layer and a stationary planar drop of electrolyte) are considered. It is shown that the method derived from Liu *et al.* [12] gives accurate predictions, whereas the delta function method exhibits an unphysical step-change in the electrical potential at the interface Finally, the extended algorithm of Berry *et al.* [1] is applied to the breakup of an unstable charged water drop in air. Predictions for this illustrative case are consistent with related experimental data [13].

References

[1] Berry, J.D., Davidson, M.R. & Harvie, D.J.E., A multiphase electrokinetic flow model for electrolytes with liquid/liquid interfaces. *J. Computational Physics*, **251**, pp. 209–222, 2013.
[2] Saville, D.A., Electrohydrodynamics: The Taylor-Melcher leaky dielectric model. *Annual Review of Fluid Mechanics*, **29**, pp. 27–64, 1997.
[3] Lac, E. & Homsy, G.M., Axisymmetric deformation and stability of a viscous drop in a steady electric field. *J. Fluid Mechanics*, **590**, pp. 239–264, 2007.
[4] Notz, P.K. & Basaran, O.A., Dynamics of drop formation in an electric field. *J. Colloid and Interface Science*, **213**, pp. 218–237, 1999.
[5] Hua, J., Lim, L.K. & Wang, C-H., Numerical simulation of deformationmotion of a drop suspended in viscous liquids under influence of steady electric fields. *Physics of Fluids*, **20**, 113302, 2008.
[6] Ghazian, O., Adamiak, K. & Castle, G.S.P., Numerical simulation of electrically deformed droplets less conductive than ambient fluid. *Colloids and Surfaces A: Physicochem. and Eng. Aspects*, **423**, pp. 27–34, 2013.

[7] Ferrera, C., Lopez-Herrera, J.M., Herrada, M.A., Montanero, J.M. & Acero, A.J., Dynamical behavior of electrified pendant drops. *Physics of Fluids*, **25**, 012104, 2013.
[8] Zholkovskij, E.K., Masliyah, J.H. & Czarnecki, J., An electrokinetic model of drop deformation in an electric field. *J. Fluid Mechanics*, **472**, pp. 1–27, 2002.
[9] López-Herrera, J.M., Popinet, S. & Herrada, M.A., A charge-conservative approach for simulating electrohydrodynamic two-phase flows using volume-of-fluid. *J. Computational Physics*, **230**, pp. 1939–1955, 2011.
[10] Harvie, D.J.E., Rudman, M. & Davidson, M.R., Parasitic current generation in combined level set and volume of fluid immiscible fluid simulations. *ANZIAM J.*, **48**, pp. C661–C676, 2008.
[11] Harvie, D.J.E., Biscombe, C.J.C. & Davidson, M.R., Microfluidic circuit analysis I: Ion current relationships for thin slits and pipes. *J. Colloid & Interface Science*, **365**, pp. 1–15, 2012.
[12] Liu, X-D, Fedkiw, R.P. & Kang, M., A boundary condition capturing method for Poisson's equation on irregular domains. *J. Computational Physics*, **160**, pp. 151–178, 2000.
[13] Giglio, E., Gervais, B., Rangama, J., Manil, B. & Huber, B.A., Shape deformations of surface-charged microdroplets. *Physical Review E*, **77**, 036319, 2008.